analytical chemistry

Perspective

pubs.acs.org/ac

Imaging Mass Spectrometry on the Nanoscale with Cluster Ion Beams

Nicholas Winograd*

Department of Chemistry, Penn State University, University Park, Pennsylvania 16875, United States

ABSTRACT: Imaging with cluster secondary ion mass spectrometry (SIMS) is reaching a mature level of development. Using a variety of molecular ion projectiles to stimulate desorption, 3-dimensional imaging with the selectivity of mass spectrometry can now be achieved with submicrometer spatial resolution and <10 nm depth resolution. In this Perspective, stock is taken regarding what it will require to routinely achieve these remarkable properties. Issues include the chemical nature of the projectile, topography formation, differential erosion rates, and perhaps most importantly, ionization efficiency. Shortcomings of existing instrumentation are also noted. Speculation about how to successfully resolve these issues is a key part of the discussion.

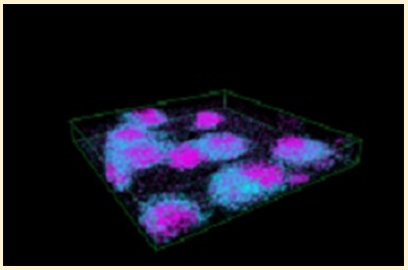

The emergence of mass spectrometry imaging has, in recent years, allowed chemical composition to be resolved with unprecedented spatial resolution and sensitivity. This capability has had implications not only for bioimaging but also for characterizing polymer surfaces, medical devices, electronic components, and organic light emitting diodes (OLEDs). Initially, this type of measurement was limited to energetic ion beam induced desorption experiments emanating from the secondary ion mass spectrometry (SIMS) community.[1] Although molecular information is obtainable with this method, significant beam-induced chemical fragmentation causes experimental complications and often makes spectral interpretation problematic. More recently, imaging using focused laser beams to initiate molecular desorption has become widespread using MALDI[2] or laser ablation with electrospray postionization where fragmentation is much more controllable.[3] Other soft desorption probes that can be spatially confined have also been tested in the imaging mode including desorption electrospray ionization (DESI).[4]

Here, the focus is on molecular SIMS. It is valid to question the efficacy of this approach, however, in light of the transformational advances associated with related mass spectrometry imaging motifs where molecular fragmentation is much less pronounced. As I shall try to show, there are critical operational modes for SIMS that put it in a unique space for materials characterization. These modes include the ability to acquire chemical information specific to the surface layers of a sample and to perform 3-dimensional imaging with submicrometer spatial resolution and nanometer-scale depth resolution. This approach is distinct from nanoSIMS where the energetic ion beam intentionally fragments the molecules to small fragments which are distinguished using stable isotope labeling.[5]

The reason d'être for this Perspective stems from the remarkable developments associated with primary ion cluster projectiles for SIMS experiments. About 10 years ago, I penned a report for *Analytical Chemistry* entitled "The Magic of Cluster SIMS", espousing the virtues of C_{60} as a projectile.[6] At that time, SIMS researchers were rapidly shifting their emphasis from atomic projectiles like Ar^+ and Ga^+ to cluster projectiles. It was clear then that when many atoms are involved in a collision with the surface, the energy per atom is reduced proportionately and the incident energy is deposited closer to the surface where it most effectively stimulates desorption.[7] In addition, there was some evidence that these clusters initiated much less subsurface damage than atomic projectiles. Cluster ion beams could be employed to erode material from the sample in a highly controlled fashion, allowing molecular composition to be determined in depth with a resolution of less than 20 nm.[8] In addition, these beams are readily focused to a submicrometer spot, allowing much higher spatial resolution than the desorption techniques mentioned above. Hence, this new paradigm holds out the enticing prospect of acquiring molecule-specific images of a range of materials with no special pretreatment and in 3 dimensions. The ability for molecular depth profiling, molecular surface analyses, and submicrometer molecular imaging is the unique characteristic that spurs continued interest in instrumental improvements, better fundamental understanding, and unusual applications. With this perspective in mind, the goal here is to reflect upon key discoveries that have led to current capabilities, highlight critical areas of difficulty that prevent further advances, and speculate about how these roadblocks can be cleared away.

■ CLUSTER BEAMS AND THEIR IMPLICATIONS

Today, the development of the protocols necessary to implement 3-dimensional imaging has advanced at a remarkable pace.[9] Virtually every SIMS lab has implemented cluster ion beams of one type or another. The situation is complicated,

Received: September 29, 2014
Accepted: December 2, 2014
Published: December 2, 2014

   dx.doi.org/10.1021/ac503650p | *Anal. Chem.* 2015, 87, 328−333

however, since there are a wide range of cluster projectiles, each with a particular advantage for a particular aspect of the measurement. The liquid metal ion gun, for example, is favored for high spatial resolution and brightness since the ions are emitted from a point source. Bismuth is the favored projectile since it has material properties that allow it to be focused to a spot well-below 100 nm.[10] In addition, Bi readily forms clusters during the emission process with Bi_3^+ being the most popular species. Another approach is to directly ionize a molecule by conventional electron impact with 20−70 eV electrons and to focus the extracted primary molecular ion using lenses and apertures. This is the approach used for the C_{60}^+ ion source mentioned above.[11] A major downside is that focusing is difficult due to the relatively large size of the ionization region. Although spot sizes of 250 nm have been reached with this approach, the extensive use of apertures greatly reduces the beam current. The upside is that a wide range of molecular species can be employed to optimize molecular desorption, ionization, or spatial resolution. In addition, it may be possible to utilize both the kinetic energy of the cluster for desorption and subsequent chemical reactions that may occur between the cluster components and the sample. Possible chemical reactions include the formation of volatile intermediates and ionization via proton attachment. A summary of some of the most intensely studied cluster projectiles is shown in Table 1.

Table 1. Summary of a Few SIMS Projectiles Applicable to Imaging Currently in Play, with an Indication of the Key Proponents of Each

projectile	m/z	proponent(s)	imaging
SF_5^+	127	Appelhans and Delmore,[12] Gillen and co-workers[13]	10 μm
Au_3^+, Bi_3^+	591−627	Vickerman and co-workers,[14] ION-TOF[10]	<100 nm
Au_{400}^{4+}	19,700	Schweikert and co-workers[15]	single impact
C_{60}^+, C_{60}^{+2}, C_{60}^{+++}	720	Vickerman and co-workers,[11] Winograd[6]	250 nm
Ar_{2500}^+	100,000	Matsuo and co-workers[16]	1−10 μm
$(H_2O)_{2000}$	36,000	Vickerman and co-workers[17]	10 μm
liquid droplets	massive	Cooks et al. and DESI[4]	100 μm

The development of the argon gas cluster ion beam (GCIB) shown in Table 1 deserves special mention in this Perspective. This source has been of interest to the community for many years after initial experiments reported by the Matsuo group at Kyoto University.[18] Using supersonic expansion of high pressure argon gas through a nozzle, clusters of up to 10,000 argon atoms could be prepared and ionized by the electron impact method noted above. When employed as a SIMS primary ion, this projectile was shown to desorb biomolecules with much less fragmentation than produced by other smaller clusters. The depth resolution in molecular depth profiling experiments was also much improved.[19] Even so, the source was not employed by other groups due to design complexity. About 5 years ago, however, several instrument companies managed to produce a compact design that could be retrofitted onto existing TOF-SIMS instruments. Interest in the new source has been phenomenal, with widespread adoption by the community.

MOLECULAR DEPTH PROFILING AND TOPOGRAPHY

One of the first challenges for molecular depth profiling and 3-dimensional imaging experiments is to determine the depth scale during ion-beam induced erosion. From the mass spectrometry side, the number of primary ions is easily determined simply by measuring the beam current. The tougher part is to determine how much material is removed during each impact, and if this amount changes during the experiment due to different material properties, how does one correct for such effects? A useful approach for simple systems is to create a crater with the primary ion beam and measure the volume of the crater using atomic force microscopy (AFM). Very accurate yield measurements can be obtained with AFM on well-behaved samples, and much has been learned about the physics of the desorption process from these measurements. A typical crater is shown in Figure 1. Not only is it easy to calculate the volume, but it is possible to acquire information about any topography that may form during the erosion process. In some instances, the amount of material can be determined by a simple weight loss measurement using the quartz crystal microbalance.[20]

Any roughening of the crater floor will introduce uncertainty in the depth measurement and will degrade the ultimate depth resolution. Fortunately, using most cluster projectiles, the microscopic roughness tends to decrease or at least to remain only a few nanometers, as a function of bombardment fluence. This observation is nicely reproduced using computer simulations of the sputtering event, which suggest that the rms roughness varies from 1 to 4 nm, depending upon projectile, angle of incidence, and kinetic energy. An example of how these simulations reveal nanoscopic roughness is shown in Figure 2.[22] Since the roughness often develops along the

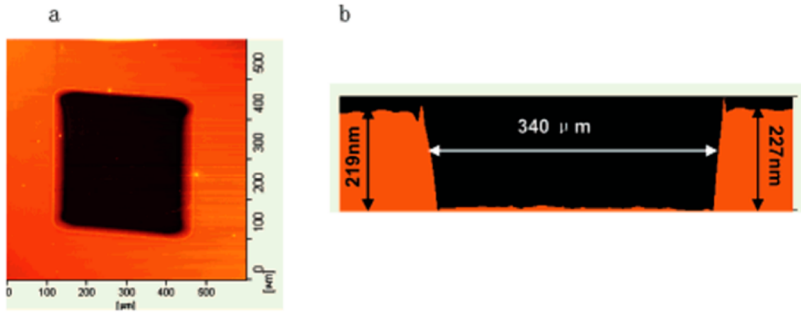

Figure 1. AFM images of a typical C_{60}^+ depth profile into a film of trehalose deposited onto silicon. The crater is approximately 340 μm square and 220 nm deep. Note the small amount of roughness at the crater bottom. (a) top-down view; (b) cross section view. Reprinted from ref 21. Copyright 2006 American Chemical Society.

dx.doi.org/10.1021/ac503650p | Anal. Chem. 2015, 87, 328−333

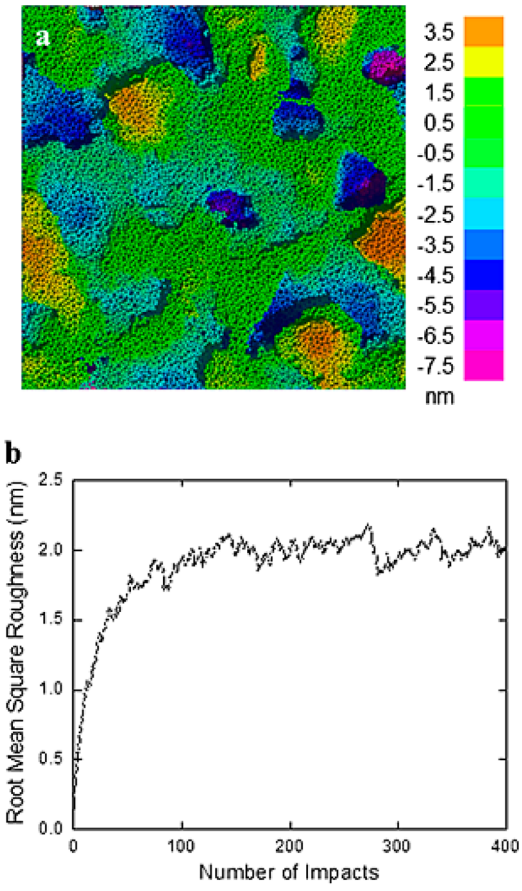

Figure 2. Computer simulations of the sputtering of a silicon target by 10 keV C_{60}^+ after 300 individual impacts. The topography is shown in (a) with yellow and orange indicating material above the surface, while purple and blue are atoms in craters below the surface. The evolution of roughness with impacts is shown in (b). Reprinted with permission from ref 22. Copyright 2013 John Wiley & Sons, Inc.

direction of the impact azimuthal angle for oblique angles of incidence, rotation of the sample during erosion has been suggested and shown to be a viable approach to reducing any topography formation even further.[23]

MOLECULAR DEPTH PROFILING OF HYBRID MATERIALS

Fundamental studies of molecular depth profiling very quickly revealed a critical problem. Bombardment of organic materials with cluster ion beams almost always occurs with a yield volume an order of magnitude larger than for inorganic materials such as metals or metal oxides. For example, the sputtering yield of cholesterol was found to be 274 nm^3 per C_{60} impact, while that of Au was found to be only 2.2 nm^3 under similar conditions.[24] In addition, when the metal is on top of the organic layer, it is observed to implant into the organic matrix, resulting in a reduced sputtering yield, increased molecular fragmentation, and an increase in the thickness of a beam-induced altered layer at the eroding surface.

A very important application of molecular depth profiling is the characterization of organic light emitting diode (OLED) devices. As it turns out, molecular depth profiles of two important OLED organic components, 4,4′-bis[*N*-(1-naphthyl-1-)-*N*-phenyl- amino]-biphenyl (NPB) and aluminum tris(8-hydroxyquinolate) (Alq_3), yield nearly artifact-free results.[25] The depth resolution of Alq_3 marker layers embedded in an NPB matrix is ∼10 nm as shown in Figure 3. The actual device, however, is overcoated with a thin layer of Al. In order to successfully depth profile through these layers, the Al coating must be physically removed at the start, typically by pulling it off with scotch tape. One could imagine that any hybrid material would yield similar artifacts. Interestingly, one approach to resolving the problem has involved depth profiling by cobombardment with a high energy C_{60}^+ probe and a very low energy Ar^+ probe.[26] With this configuration, the Al layer could be removed without complications. Although this approach has been questioned, perhaps this sort of scheme can be generalized to further broaden the scope of this type of measurement.

IMPLICATIONS FOR BIOIMAGING

Since differential erosion rates can put a damper on molecular depth profiling and 3-dimensional molecular imaging, it is logical to question whether this approach is meaningful for characterizing single biological cells. Certainly, the goal of performing this type of measurement has been a cause célèbre

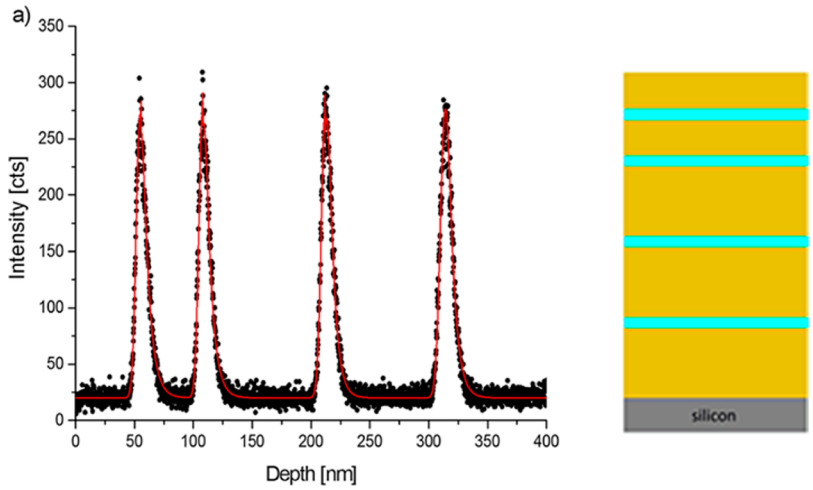

Figure 3. $[AlQ_3 + H]^+$ intensity versus depth into the structure, whose schematic is shown on the right. Alq_3 is purple, and NPB is orange. The Alq_3 layers are 3 nm thick. Reprinted with permsission from ref 25. Copyright 2014 John Wiley & Sons, Inc.

dx.doi.org/10.1021/ac503650p | *Anal. Chem.* 2015, 87, 328−333

for SIMS users since the early 1990s. More recently, however, several groups have proposed protocols for 3-dimensional measurements that again utilize the AFM to determine the depth scale in order to account for yield variations. The Castner lab has shown that, for formalin-fixed HeLa cells, the erosion rate is 4 nm per 10^{13} C_{60} ions (40 nm^3 per C_{60} impact) at 10 keV.[9b] To achieve submicrometer spatial resolution, they employed the Bi_3^+ ion source for imaging. The cells were treated with bromodeoxyuridine (BrdU), a well-known nuclear marker, to ensure that the images were representative of the intact cell. Their results show that the sputter rate is constant during the C_{60}^+ erosion, suggesting that the chemical nature of the cell is uniform enough to prevent the distortions associated with the organic/inorganic hybrid systems mentioned above. Because of the uniform erosion rate, they could apply a simple z-correction to the 2-dimensional images to create an accurate 3-dimensional representation, shown in Figure 4. This

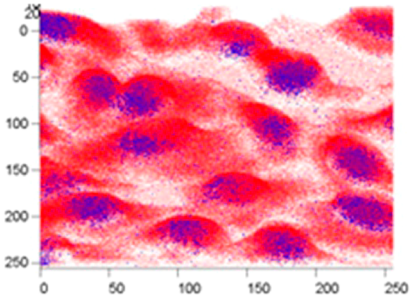

Figure 4. z-corrected images of BrdU localized within HeLa cells. The image is 202 × 202 μm^2 and contains 24 slices. The $BrdU^-$ signal is shown in blue, and the sum of $C_xH_yO_z^-$ fragment ions are shown in red. Reprinted from ref 9b. Copyright 2013 American Chemical Society.

correction is an important transformation to accurately account for the erosion of nonflat samples.[27] It is important to try to generalize these observations to other cell types and cell-preparation methods, since the assumption of uniform erosion is central to the success of this approach. For example, attempts to depth profile single biological cells with embedded TiO_x nanoparticles yield a three-dimensional image with a greatly distorted depth scale, illustrated in Figure 5.[28]

IONIZATION, IONIZATION, AND IONIZATION!

In addition to understanding the physical aspects of molecular sputtering, it is equally important to maximize molecular ionization during sputtering and to minimize the notorious matrix ionization effects. It is generally stated that the probability of ionization for typical organic molecules is in the range of 1 molecule in 10^8 to 1 molecule in 10^4, although values outside this range can be found. Ionization is a rare event, with most of the sputtered flux consisting of neutral molecules and fragments. This fact obviously has an enormous influence on ultimate sensitivity, but perhaps even more importantly, it limits the spatial resolution that can be achieved. There are only a million molecules (of typical size) per layer per square micrometer. If several layers can be added together during erosion, the sample volume could approach a billion molecules. With an ionization probability of 1 part in 10^8, however, it is clear that there simply is not enough material to detect a signal, even with the most efficient mass spectrometers, as the pixel size decreases into the nanometer range.

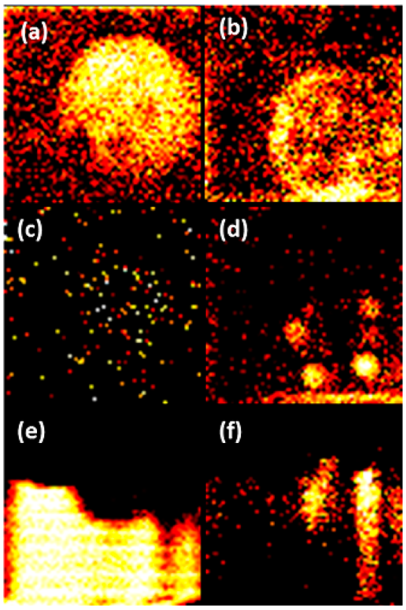

Figure 5. C_{60}-SIMS images of a tetrahymena single cell with implanted TiO_2 nanoparticles. The image in (a) is the phosphatidylcholine signal (m/z 184.1) on the surface of a frozen hydrated cell, using the $x-y$ plane. The image in (b) shows the m/z 184.1 signal after etching through the cell surface. The corresponding TiO^+ signals are shown in panels (c) and (d). To show the effect of differential sputtering rates, $x-z$ images are plotted in (e) and (f). The (e) image shows the Si substrate, and the (f) panel shows the distorted Ti particle, which sputters much more slowly than the cellular material. The field of view here is 70 × 70 μm^2. Reprinted with permission from ref 28. Copyright 2014 John Wiley & Sons, Inc.

The ionization problem effects the situation in other ways as well. With smaller cluster projectiles such as Bi_3^+, ions are produced in greater quantity, but more molecules are fragmented, reducing the molecular ionization efficiency. With the larger clusters, such as the GCIB beams shown in Table 1, molecular desorption is very efficient, but the "softness" of the ionization means that the ionization efficiency is poor. We are faced with a classic conundrum. It seems that the only way out is to figure out new ways to enhance molecular ionization during projectile impact. Implementation of matrices as with MALDI might be helpful in this regard,[29] but this approach is not compatible with molecular depth profiling and 3-dimensional imaging, obviating much of the uniqueness of modern day SIMS. Another strategy is to tinker with the chemistry of the GCIB projectile, itself. That is the thinking behind the development of proton rich GCIBs such as H_2O[17] or doped GCIBs containing hydrogen-rich small molecules such as CH_4.[30] Presumably, these H atoms wind up as embedded protons after projectile impact to enhance $[M + H]^+$ formation. Finally, it is possible to employ both ion sources simultaneously. The Bi_3^+ source is used for spectral acquisition and imaging, while the GCIB is employed purely for erosion and depth information.[31] These approaches all appear promising with ionization enhancements of an order of magnitude or so, but more is needed.

The other remaining difficulty with ionization involves dreaded matrix ionization effects. For organic molecules, there can be interactions between sputtered ions that enhance one component and suppress another. Since the ionization mechanism usually involves proton attachment, the magnitude

dx.doi.org/10.1021/ac503650p | Anal. Chem. 2015, 87, 328−333

of these effects is often related to the relative gas phase basicity of the two components. It has been shown that the intensity of a drug molecule in various portions of brain tissue is high where it should be low and low where it should be high due to interactions between the drug and the lipid components in the tissue.[32] More recent studies have investigated ion suppression effects quantitatively using thermally evaporated thin film structures of multicomponent organic species. These experiments showed that low molecular weight fragment ions exhibited much smaller matrix effects than the heavier molecular ions. In addition, a simple model was introduced which, using pure component standards as reference, allowed correction for matrix effects and allowed accurate compositional analysis of binary organic mixtures.[33] This approach represents an important beginning for unraveling these effects in more complex materials such as biological cells and tissue.

IMPLICATIONS FOR INSTRUMENTATION

These recent developments in cluster-SIMS have altered the instrumentation landscape. Prior to molecular depth profiling and 3-dimensional imaging, instrumentation was designed for optimum transmission using time-of-flight mass analyzers. With this configuration, the ion beam dose is kept small to avoid the accumulation of chemical damage on the sample surface, although detection efficiency is maximized.[34] The primary ion beam is pulsed with a duty cycle of ~1 part in 10^6. The requirement for a pulsed beam also means that high spatial resolution and high mass resolution is not easily obtained at the same time. With the lifting of the dose restriction, the use of modern mass spectrometer designs has become feasible. A C_{60} source has been coupled to a hybrid triple-quadrupole orthogonal TOF.[35] This design utilizes a continuous primary ion beam and provides direct access to tandem mass spectrometry studies. The continuous ion beam is important since the duty cycle is, in principle, 100%, and high spatial resolution and high mass resolution can be achieved at the same time. Another innovative design has appeared which employs a shaped-field buncher to time focus a section of the continuous beam which is accelerated into a harmonic reflectron.[36] Other groups are working on using Fourier transform mass analyzers[37] to achieve ultrahigh mass resolution.

There is now a major initiative that addresses many of the issues raised here, with the goal of increasing the ionization efficiency by 2 orders of magnitude and of providing label-free molecular imaging in 3 dimensions with 50 nm spatial resolution. (http://www.npl.co.uk/news/3d-nanosims-label-free-molecular-imaging) The initiative, led by researchers at the National Physical Lab in the UK, involves a collaboration between two prominent instrument companies, industry, as well as academic institutions in both the UK and the US. The strategy targets the two-ion-gun approach to maximize ionization with reduced damage, laser postionization to maximize ionization efficiency, and the implementation of an orbitrap device for ultrahigh mass resolution with tandem mass spectrometry capabilities. The goal of this new instrument is to identify where drugs go at the single cell level, even within specific organelles.

WHAT NEXT?

From this Perspective, it is hopefully clear that a continuous stream of technical developments have relentlessly improved the characteristics of SIMS, bringing it to the present advanced state. When looking at the 50 year history of contributions, it is easy to see that SIMS was an important precursor to the modern revolution in mass spectrometry starting with the invention of MALDI and electrospray methods in the 1980s.[38] This history suggests that more advances are still to come. As noted above, there is still no consensus about the most effective primary cluster projectile where ionization efficiency, depth resolution, and spatial resolution are optimized. Depth scale issues and matrix ionization effects seem destined to be worked out to most people's satisfaction. The elephant in the room remains to be the poor ionization efficiency, which ultimately limits spatial resolution. Clever breakthroughs are urgently needed to resolve this problem, which will require better fundamental understanding of the basic ionization mechanisms themselves. For example, can the chemistry of the projectile be optimized to enhance ionization during a single impact event, or will chemical modification of the sample surface through many impacts be required?

AUTHOR INFORMATION

Corresponding Author

*E-mail: nxw@psu.edu.

Notes

The author declares no competing financial interest.

ACKNOWLEDGMENTS

This study was financially supported by the National Institutes of Health (Grant No. 9R01 GM113746-20A1), the National Science Foundation (Grant No. CHE-0908226), and the Department of Energy (Grant No. DE-FG02-06ER15803)

REFERENCES

(1) Castaing, R.; Jouffrey, B.; Slodzian, G. *C. R. Hebd. Seances Acad. Sci.* **1960**, *251* (8), 1010−1012.
(2) Caprioli, R. M.; Farmer, T. B.; Gile, J. *Anal. Chem.* **1997**, *69* (23), 4751−4760.
(3) Nemes, P.; Vertes, A. *Anal. Chem.* **2007**, *79* (21), 8098−8106.
(4) Cooks, R. G.; Ouyang, Z.; Takats, Z.; Wiseman, J. M. *Science* **2006**, *311* (5767), 1566−1570.
(5) (a) Steinhauser, M. L.; Bailey, A. P.; Senyo, S. E.; Guillermier, C.; Perlstein, T. S.; Gould, A. P.; Lee, R. T.; Lechene, C. P. *Nature* **2012**, *481* (7382), 516−U131. (b) Zhang, D. S.; Piazza, V.; Perrin, B. J.; Rzadzinska, A. K.; Poczatek, J. C.; Wang, M.; Prosser, H. M.; Ervasti, J. M.; Corey, D. P.; Lechene, C. P. *Nature* **2012**, *481* (7382), 520−U137.
(6) Winograd, N. *Anal. Chem.* **2005**, *77* (7), 142A−149A.
(7) Mahoney, C. M.; Roberson, S. V.; Gillen, G. *Anal. Chem.* **2004**, *76* (11), 3199−3207.
(8) Gillen, G.; Fahey, A.; Wagner, M.; Mahoney, C. *Appl. Surf. Sci.* **2006**, *252* (19), 6537−6541.
(9) (a) Wucher, A.; Cheng, J.; Winograd, N. *Anal. Chem.* **2007**, *79* (15), 5529−5539. (b) Brison, J.; Robinson, M. A.; Benoit, D. S. W.; Muramoto, S.; Stayton, P. S.; Castner, D. G. *Anal. Chem.* **2013**, *85* (22), 10869−10877.
(10) Touboul, D.; Kollmer, F.; Niehuis, E.; Brunelle, A.; Laprevote, O. *J. Am. Soc. Mass Spectrom.* **2005**, *16* (10), 1608−1618.
(11) Weibel, D.; Wong, S.; Lockyer, N.; Blenkinsopp, P.; Hill, R.; Vickerman, J. C. *Anal. Chem.* **2003**, *75* (7), 1754−1764.
(12) Appelhans, A. D.; Delmore, J. E. *Anal. Chem.* **1989**, *61* (10), 1087−1093.
(13) Fuoco, E. R.; Gillen, G.; Wijesundara, M. B. J.; Wallace, W. E.; Hanley, L. *J. Phys. Chem. B* **2001**, *105* (18), 3950−3956.
(14) Davies, N.; Weibel, D. E.; Blenkinsopp, P.; Lockyer, N.; Hill, R.; Vickerman, J. C. *Appl. Surf. Sci.* **2003**, *203*, 223−227.
(15) Li, Z.; Verkhoturov, S. V.; Schweikert, E. A. *Anal. Chem.* **2006**, *78* (21), 7410−7416.

(16) Toyoda, N.; Matsuo, J.; Aoki, T.; Yamada, I.; Fenner, D. B. *Appl. Surf. Sci.* **2003**, *203*, 214−218.
(17) Sheraz, S.; Barber, A.; Fletcher, J. S.; Lockyer, N. P.; Vickerman, J. C. *Anal. Chem.* **2013**, *85* (12), 5654−5658.
(18) Ninomiya, S.; Nakata, Y.; Honda, Y.; Ichiki, K.; Seki, T.; Aoki, T.; Matsuo, J. *Appl. Surf. Sci.* **2008**, *255* (4), 1588−1590.
(19) Lee, J. L. S.; Ninomiya, S.; Matsuo, J.; Gilmore, I. S.; Seah, M. P.; Shard, A. G. *Anal. Chem.* **2010**, *82* (1), 98−105.
(20) Szakal, C.; Kozole, J.; Russo, M. F.; Garrison, B. J.; Winograd, N. *Phys. Rev. Lett.* **2006**, *96* (21), 216104.
(21) Cheng, J.; Wucher, A.; Winograd, N. *J. Phys. Chem. B* **2006**, *110* (16), 8329−8336.
(22) Cook, E. L.; Krantzman, K. D.; Garrison, B. J. *Surf. Interface Anal.* **2013**, *45* (1), 93−96.
(23) Rading, D.; Moellers, R.; Kollmer, F.; Paul, W.; Niehuis, E. *Surf. Interface Anal.* **2011**, *43* (1−2), 198−200.
(24) Shen, K.; Mao, D.; Garrison, B. J.; Wucher, A.; Winograd, N. *Anal. Chem.* **2013**, *85*, 10565−10572.
(25) Holzweber, M.; Shard, A. G.; Jungnickel, H.; Luch, A.; Unger, W. E. S. *Surf. Interface Anal.* **2014**, DOI: 10.1002/sia.5429.
(26) Lin, W.-C.; Wang, W.-B.; Lin, Y.-C.; Yu, B.-Y.; Chen, Y.-Y.; Hsu, M.-F.; Jou, J.-H.; Shyue, J.-J. *Org. Electron.* **2009**, *10* (4), 581−586.
(27) Breitenstein, D.; Rommel, C. E.; Mollers, R.; Wegener, J.; Hagenhoff, B. *Angew. Chem., Int. Ed.* **2007**, *46* (28), 5332−5335.
(28) Angerer, T. B.; Fletcher, J. S. *Surf. Interface Anal.* **2014**, DOI: 10.1002/sia.5444.
(29) Eijkel, G. B.; Kaletas, B. K.; van der Wiel, I. M.; Kros, J. M.; Luider, T. M.; Heeren, R. M. A. *Surf. Interface Anal.* **2009**, *41* (8), 675−685.
(30) Wucher, A.; Tian, H.; Winograd, N. *Rapid Commun. Mass Spectrom.* **2014**, *28* (4), 396−400.
(31) Rading, D.; Moellers, R.; Cramer, H. G.; Niehuis, E. *Surf. Interface Anal.* **2013**, *45* (1), 171−174.
(32) Jones, E. A.; Lockyer, N. P.; Kordys, J.; Vickerman, J. C. *J. Am. Soc. Mass Spectrom.* **2007**, *18* (8), 1559−1567.
(33) Shard, A. G.; Spencer, S. J.; Smith, S. A.; Havelund, R.; Gilmore, I. S. *Int. J. Mass Spectrom.* **2014**, DOI: 10.1016/j.ijms.2014.06.027.
(34) Iltgen, K.; Bendel, C.; Benninghoven, A.; Niehuis, E. *J. Vac. Sci. Technol., A: Vac., Surf. Films* **1997**, *15* (3), 460−464.
(35) Carado, A.; Kozole, J.; Passarelli, M.; Winograd, N.; Loboda, A.; Wingate, J. *Appl. Surf. Sci.* **2008**, *255* (4), 1610−1613.
(36) Hill, R.; Blenkinsopp, P.; Thompson, S.; Vickerman, J.; Fletcher, J. S. *Surf. Interface Anal.* **2011**, *43* (1−2), 506−509.
(37) Smith, D. F.; Kiss, A.; Leach, F. E.; Robinson, E. W.; Pasa-Tolic, L.; Heeren, R. M. A. *Anal. Bioanal. Chem.* **2013**, *405* (18), 6069−6076.
(38) Vickerman, J. C.; Winograd, N. *Int. J. Mass Spectrom.* **2014**, DOI: 10.1016/j.ijms.2014.06.021.